Preprints (www.preprints.org) | NOT PEER-REVIEWED | Posted: 18 September 2018 doi:10.20944/preprints201809.0341.v1

Peer-reviewed version available at *Int. J. Mol. Sci.* **2018**, *19*, 3566; doi:10.3390/ijms19113566

Article

Relative contribution of PIN-containing secretory vesicles and plasma membrane PINs to the directed auxin transport: theoretical estimation

Sander Hille[1†], Maria Akhmanova[2†], Matouš Glanc[2,3], Alexander Johnson[2] and Jiří Friml[2*]

[1] Mathematical Institute, Faculty of Science, Leiden University, Leiden, The Netherlands; shille@math.leidenuniv.nl
[2] Institute of Science and Technology (IST) Austria, Am Campus 1, Klosterneuburg, Austria; axmahoba@gmail.com (M.A.), matous.glanc@gmail.com (M.G.)
[3] Dpt. Experimental Plant Biology, Faculty of Science, Charles University, Prague, Czechia
[†] These authors contributed equally to this work
[*] Correspondence: jiri.friml@ist.ac.at; Tel.: +43 2243 9000 5401

Abstract: Intercellular transport of auxin is driven by PIN-formed (PIN) proteins. PINs are localized at the plasma membrane (PM) and on constitutively recycling endomembrane vesicles. Therefore, PINs can mediate auxin transport either by direct translocation across the PM or by pumping it into secretory vesicles (SVs), leading to its secretory release upon fusion with the PM. Which of these two mechanisms dominates is a matter of debate. Here we addressed the issue with a mathematical modeling approach. We demonstrate that the efficiency of secretory transport depends on SV size, half-life of PINs on the PM, pH, exocytosis frequency and PIN density. 3D-SIM microscopy was used to determine PIN density on the PM. Combing this data with published values of the other parameters, we show that the transport activity of PINs in SVs would have to be at least 1000x greater than on the PM in order to produce a comparable macroscopic auxin transport. If both transport mechanisms operated simultaneously and PINs were equally active on SVs and PM, the contribution of secretion to the total auxin flux would be negligible. In conclusion, while secretory vesicle-mediated transport of auxin is intriguing and theoretically possible model, it unlikely to be a major mechanism of auxin transport in planta.

Keywords: Auxin; Polar Auxin Transport; PIN transporters; Secretion; 3D-SIM microscopy; Mathematical modeling

1. Introduction

The plant hormone auxin (IAA) is subject to intercellular Polar Auxin Transport (PAT) mediated by diffusion and the action of efflux and influx carriers. PAT generates local auxin maxima that are crucial for a plethora of developmental processes [1]. Therefore, studies into the mechanism of auxin transport and its regulation have had a prominent place in the auxin field. Auxin maxima-driven developmental events depend on the activity of the PIN-FORMED (PIN) IAA efflux carriers, which provide directionality to intercellular IAA transport through their asymmetric subcellular localization [1,2]. The PIN proteins constitutively cycle between the plasma membrane (PM) and endosomal compartments [3–5], and the developmental importance of this energetically demanding phenomenon has not been unequivocally explained. Three hypotheses have been suggested to explain the requirement of PIN recycling: 1) Recycling enables rapid relocation of PINs and thereby the rapid redirection of auxin transport; 2) PINs serve as IAA transceptors (transporters and receptors at the same time) and their recycling is important for the process of signal transduction; and 3) the PIN-containing secretory vesicles (SVs) are filled with auxin, which is released into the apoplast upon fusion of the SV with the PM. This process is analogous to neurotransmitter release in animals, and is important for the transport of auxin as suggested by previous reports [6,7] (Figure 1).

© 2018 by the author(s). Distributed under a Creative Commons CC BY license.

Preprints (www.preprints.org) | NOT PEER-REVIEWED | Posted: 18 September 2018 doi:10.20944/preprints201809.0341.v1

Peer-reviewed version available at Int. J. Mol. Sci. 2018, 19, 3566; doi:10.3390/ijms19113566

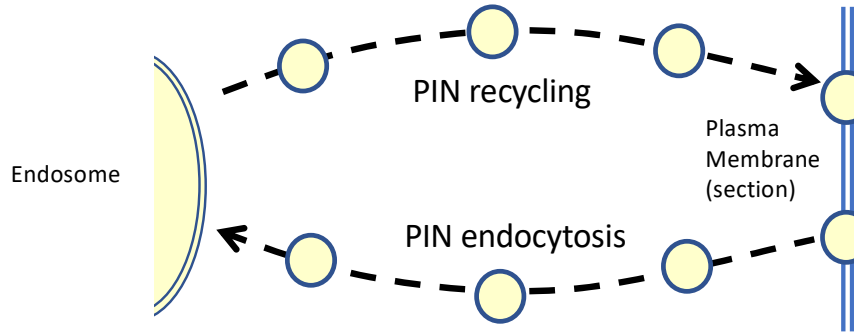

Figure 1. Schematics of PIN endomembrane trafficking.

Several studies claimed to have proven the vesicular transport of IAA [8–10]. However, the validity of the evidence presented in most of these studies has been questioned by many researchers in the field, and thus the hypothesis of vesicular transport of auxin remains controversial [11,12]. A major reason this controversy exists is the inability to uncouple vesicular trafficking from PIN occurrence at the PM using existing cell biology methods. For example, if one could genetically or pharmacologically completely and specifically block the movement of PIN-containing secretory vesicles, it would be impossible to conclude whether the resulting reduction in auxin transport was caused by the lack of IAA secreting vesicles or by the lack of PINs at the PM.

Here, we have constructed a simple mathematical model to estimate the parameters under which *auxin transport by intracellular vesicles could explain the measured net flux values of PAT*. We show that vesicular transport model would require at least 1000 times greater PIN activity than the conventional PM transport model to generate the same net flux values.

2. Results

2.1 Model assumptions: PINs can be active on the endomembrane vesicles exclusively or in addition to their activity on the PM

PAT is characterized by the sustained velocity of auxin over long distances (several millimeters, which is much greater than a typical cell length). The magnitude of this velocity is in the range of $1 \div 10 \frac{\mu m}{s}$ for different species and different types of plant tissue [13]. Arabidopsis root epidermal cells serve as a useful example because many of the physiological parameters which influence the PAT, and thus used in our calculations, have been experimentally measured in this cell type. Furthermore, vesicular auxin transport has been proposed to play a role in the transition zone of the root [8]. Thus, we chose to apply our model to this tissue. In the roots auxin is transported towards the root tip inside the central cells (stele), whereas in the outer cell layer (lateral root cap cells and epidermal cells) it is transported in the reverse direction: from the root tip towards the shoot [14]. The velocity of this directed transport in Arabidopsis roots was found to be $v_{PAT} = 2 \div 3 \frac{\mu m}{s}$[15]. We therefore assume that $v_{PAT} \geq 1 \frac{\mu m}{s}$ in the epidermal cells in the root transition zone and estimated the permeability of PINs needed to yield this value.

In our model we consider only secretory/recycling vesicles (SVs) that fuse with the PM, and consider these secretory vesicles as the method of PIN delivery from the endosome to the PM. For such auxin-transporting vesicles we considered two hypothetical scenarios: 1) PINs transport auxin exclusively in these endomembrane vesicles; and 2) PINs transport auxin both in the vesicles and on the PM. The auxin permeability of a PIN-containing membrane (P_{PIN}) remains undetermined. However, P_{PIN} has been calculated previously for scenario when PINs are active solely on PM (P_{PIN}^{PM}) [16,17]. Therefore, the permeability of PINs in vesicles P_{PIN}^{v} is a readout rather than input to our

Preprints (www.preprints.org) | NOT PEER-REVIEWED | Posted: 18 September 2018 doi:10.20944/preprints201809.0341.v1

Peer-reviewed version available at *Int. J. Mol. Sci.* **2018**, *19*, 3566; doi:10.3390/ijms19113566

calculations. We calculated 1) the relative values of permeability P_{PIN}^{v} and the *individual activity of PINs proteins* needed for the vesicular transport model to generate the same net flux as the PM model and 2) the relative contribution of the vesicular transport to the net flux, assuming that PINs activity is the same in the vesicles and in the PM.

2.2 Short summary of model results

1) For the case when only vesicular PINs are actively transporting auxin, we derived equations for auxin accumulation inside the vesicles. The auxin accumulation ratio depends on the permeability of the vesicle membrane to auxin due to PINs (P_{PIN}^{v}). At the same time, it governs the amount of auxin released by this mechanism. Therefore, we relate macroscopic auxin transport velocity (v_{PAT}) to P_{PIN}^{v} and calculated the coefficient of proportionality between these variables for the physiological values of the other parameters: $\boldsymbol{P_{PIN}^{v-only} \geq 40 \cdot v_{PAT}}$.

However, if PINs are only active on the PM, then PINs permeability $\boldsymbol{P_{PIN}^{PM-only} \simeq v_{PAT}}$ [16]. Thus, for the minimal $v_{PAT} = 1\frac{\mu m}{s}$, as observed in epidermal root cells [13], the lower bound of permeability is $P_{PIN}^{v-only} \simeq 40\frac{\mu m}{s}$ for vesicular transport and $P_{PIN}^{PM-only} \simeq 1\frac{\mu m}{s}$ for PM transport.

Furthermore, by reducing permeability values by the density of PINs we show that the activity of individual PINs on the vesicle membrane has to be 3 orders of magnitude higher than in the scenario where they are active only on the PM, in order to produce the same PAT velocity: $\frac{p_{v-only}}{p_{PM-only}} > 4200$.

2) In the case that PINs are active both in vesicles and on the PM, the auxin flux ratio through these two mechanisms reads:

$$\frac{\Phi_{PM}}{\Phi_v} = 4200 \cdot \frac{p_{PM}}{p_v},$$

where $\frac{p_{PM}}{p_v}$ is the ratio of individual activities of PIN molecules in these domains. If activities are equal, $p_{PM} = p_v$, auxin flux through SVs contributes no more than 0.02% of the total flux.

Conclusion: The transport of auxin by vesicles is ~1000 times less efficient than through PINs active on the PM. Permeability values of PINs (P_{PIN}^{v} and P_{PIN}^{PM}) still await direct measurements, but values as high as $P_{PIN}^{v} = 40\frac{\mu m}{s}$, as estimated in our study, are unlikely. This therefore argues against vesicular transport of auxin in SVs as a major mechanism of directional auxin transport.

2.3 Detailed model description.

2.3.1. PINs active only in vesicles.

1. **How much auxin should a vesicle with active PIN contain to produce the PAT?**

1.1 Size of a vesicle.

The size of exocytotic vesicles that are considered to perform auxin transport are well known, where the dimeter of these vesicles are reported to be $d = 0.06 \div 0.08\ \mu m$ [18], and are spherical in shape (see Table 2 for corresponding surface area and volume).

Table 1. Values of parameters used in this study.

Parameter	Description	Value /Range	Ref.

Preprints (www.preprints.org) | NOT PEER-REVIEWED | Posted: 18 September 2018 doi:10.20944/preprints201809.0341.v1

Peer-reviewed version available at Int. J. Mol. Sci. 2018, 19, 3566; doi:10.3390/ijms19113566

d	Typical diameter of a vesicle	$0.06 \div 0.08\ \mu m$	[18]
$S_v = \pi d2$	Surface area of a vesicle	$1.1 \div 2.0 \cdot 10^{-2}\ \mu m^2$	
$V_v = (1/6)\pi d3$	Volume of a vesicle	$1.1 \div 2.7 \cdot 10^{-4}\ \mu m^3$	
v_{PAT}	Speed of directional IAA transport in epidermal cells of Arabidopsis root tip	$2 \div 3\ \mu m/s$	[13,15]
$\tau_{1/2}$	Half-life of PINs on the plasma membrane	$1.3 \cdot 10^4 s$	[19]
$(\rho_v)_{min}$	Minimum PIN density in a vesicle	$50 \frac{1}{\mu m^2}$	One molecule per vesicle
$(\rho_{PM})_{max}$	Maximum PIN density on a plasma membrane	$2 \cdot 10^4 \frac{1}{\mu m^2}$ $4 \cdot 10^3 \frac{1}{\mu m^2}$	Close-packing of equal spheres of 4nm radius. Estimate based on experimental data, this study.
P_{diff}(IAAH)	Diffusional permeability of IAA through membrane	0.5 μm/s	[17,20]

1.2 Biochemical constituents and transport processes. Equation for auxin concentration inside the vesicle.

The total concentration of auxin (IAA) is the mixture of anions IAA^- and protonated IAAH, and the ratio between which depends on pH of the solution:

$pH_c = 7$ in cytoplasm, ~99% of IAA^-, 1% of IAAH

$pH_v = 5.5 \div 6.5$ in vesicle, ~ 83%-98% of IAA^-, 17%-2% of IAAH

$pK_a = 4.8$ for IAA.

The fractions of IAA in anion form in cytosol and vesicle are denoted by f_{ac} and f_{av} respectively. The values were computed using

$$f_{av} = \frac{1}{1+10^{pK_a - pH_v}},$$

$$f_{ac} = \frac{1}{1+10^{pK_a - pH_c}}.$$

Thus, $(1 - f_{av})$ and $(1 - f_{ac})$ are fractions of IAAH in vesicle and cytosol respectively (see Figure 2 and Table 2 for IAA^- fractions depending on pH).

We denote

A_c - cytoplasmic concentration of auxin [mol/l],

A_v - concentration of auxin inside the vesicle [mol/l].

Preprints (www.preprints.org) | NOT PEER-REVIEWED | Posted: 18 September 2018 doi:10.20944/preprints201809.0341.v1

Peer-reviewed version available at Int. J. Mol. Sci. 2018, 19, 3566; doi:10.3390/ijms19113566

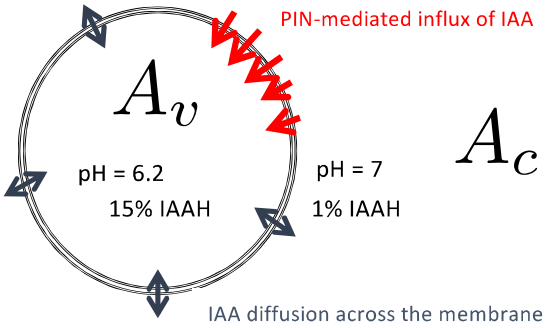

Figure 2: Scheme of auxin transport into a PIN-containing secretory vesicle

Table 2. Dependence of the accumulation ratio **R** (eq.8) and maximum number of molecules in the vesicle $\boldsymbol{N_v^{max}}$ (Eq.7) on pH in the vesicle. The last column provides lower bounds for $\frac{P_{PIN}^{v-only}}{P_{diff}}$, required to yield directional transport of auxin v_{PAT} depending on pH_v. $\boldsymbol{f_{av/c}}$ – fraction of IAA^- in the vesicle/cytoplasm, $(\boldsymbol{1-f_{av/c}})$ -fraction of IAAH in the vesicle/cytoplasm.

$\boldsymbol{pH_v}$	$\boldsymbol{f_{av}}$	$\boldsymbol{1-f_{av}}$	R *	$\boldsymbol{N_v^{max}}$	$\boldsymbol{\frac{P_{PIN}^{v-only}}{P_{diff}}}$
5.5	0.833	0.167	$6.0\cdot\frac{P_{PIN}^{v}}{P_{diff}}+0.036$ **	$0.096\cdot\frac{P_{PIN}^{v}}{P_{diff}}$	$\geq 2330\frac{s}{\mu m}\cdot v_{PAT}$
6.2	0.962	0.038	$26.2\cdot\frac{P_{PIN}^{v}}{P_{diff}}+0.16$**	$0.42\cdot\frac{P_{PIN}^{v}}{P_{diff}}$	$\geq 535\frac{s}{\mu m}\cdot v_{PAT}$
6.5	0.980	0.020	$49.7\cdot\frac{P_{PIN}^{v}}{P_{diff}}+0.3$**	$0.80\cdot\frac{P_{PIN}^{v}}{P_{diff}}$	$\geq 280\frac{s}{\mu m}\cdot v_{PAT}$
7.0	0.994 $=f_{ac}$	0.006 $=1-f_{ac}$	$166\cdot\frac{P_{PIN}^{v}}{P_{diff}}+1$**	$2.7\cdot\frac{P_{PIN}^{v}}{P_{diff}}$	$\geq 80\frac{s}{\mu m}\cdot v_{PAT}$

* For lower pH_v accumulation ratios R have lower coefficient in front of $\frac{P_{PIN}^{v-only}}{P_{diff}}$ because diffusion from the vesicle, that balances PIN-mediated influx, is higher for lower pH_v.

** Terms in gray are always much smaller than left terms and can be neglected.

Fast diffusion in the cytoplasm ($D_c = 600\ \mu m^2/s$) ensures fast mixing of IAA inside the small vesicle, that takes $\tau_{diff} \leq 10^{-6}$ s in vesicles of diameter $d \leq 100\ nm$. Thus, IAA concentration inside the vesicle can be considered homogenous and increases proportionally to the flux through the membrane:

$$\frac{dA_v}{dt} = \frac{1}{V_v} J_{in}^{net}, \qquad \text{(Eq.1)}$$

where J_{in}^{net} is the net influx of IAA into vesicle (units [mol/s]), which has two components: transport of anions IAA^- by PINs and transport of protonated neutral form $IAAH$ by diffusion through membrane:

$$J_{in}^{net} = J_{PIN}^{IAA^-} + J_{diff}^{IAAH} \qquad \text{(Eq.2)}$$

$$J_{diff}^{IAAH} = P_{diff} S_v \left((1 - f_{ac})A_c - (1 - f_{av})A_v\right) \qquad \text{(Eq.3)}$$

Preprints (www.preprints.org) | NOT PEER-REVIEWED | Posted: 18 September 2018 doi:10.20944/preprints201809.0341.v1

Peer-reviewed version available at Int. J. Mol. Sci. 2018, 19, 3566; doi:10.3390/ijms19113566

Diffusional permeability is known: $P_{diff}(\text{IAAH}) = 0.5\ \mu m/s$ [17,20]; $P_{diff}(IAA^-) \simeq \frac{P_{diff}(\text{IAAH})}{100} = 0.005\ \mu m/s$ and is considered negligible. IAAH has the same diffusional permeability P_{diff} in both directions, as seen in Eq.3.

PINs transport anions IAA- and are presumed to be permeable only in one direction (into vesicle) resulting in the unknown permeability P^v_{PIN} of the vesicular membrane. We neglect dependence of PIN-mediated influx on intravesicular auxin concentration and assume that reverse permeability is zero. By doing so, we make PINs more efficient in our considerations than they can possibly be in reality. This approach is acceptable because our aim is to find the lower bound of the permeability of PINs which is able to produce the physiologically observed PAT transport.

Thus, PIN-mediated transport is simplified to:

$$J^{IAA^-}_{PIN} = P^v_{PIN}\, S_v\, f_{ac}\, A_c \qquad \text{(Eq.4)}$$

Net total flux has thus the following form:

$$J^{net}_{in} = P^v_{PIN}\, S_v\, f_{ac}\, A_c + P_{diff} S_v\, ((1 - f_{ac})A_c - (1 - f_{av})A_v). \qquad \text{(Eq.5)}$$

Eq.1 can be rewritten as:

$$\frac{dA_v}{dt} = A_c \cdot \alpha - \lambda \cdot A_v\ , \qquad \text{(Eq.6)}$$

where

$$\alpha = \frac{P^v_{PIN}\, S_v}{V_v}\, f_{ac} + \frac{P_{diff} S_v}{V_v}(1 - f_{ac}),$$

$$\lambda = \frac{P_{diff} S_v}{V_v}(1 - f_{av}).$$

1.3 Maximum loading of vesicles with auxin is proportional to the permeability of PINs.

We assume that vesicles exist in the cytoplasm long enough that the vesicular internal auxin concentration reaches its maximum: steady state concentration A_v. It is reached at time $t >> \tau_{load} = \frac{1}{\lambda} = 4.6s$ for $pH_v = 7$ (and faster for $pH_v < 7$). We consider fully filled vesicles because our aim is to find the *minimal* requirements for the vesicular transport, and partly filled vesicles would require *higher* permeability values to produce the PAT.

At steady state, when $\frac{dA_v}{dt} = 0$, Eq.6 simplifies to:

$$A_c \cdot \alpha = \lambda \cdot A_v\ , \qquad \text{(Eq.6')}$$

Thus, number of IAA molecules (in moles) in one vesicle**:**

$$N^{max}_v = A^{max}_v \cdot V_v = A_c \cdot V_v \frac{\alpha}{\lambda}\ , \qquad \text{(Eq.7)}$$

Substituting α and λ by their expressions gives:

$$\boldsymbol{N^{max}_v = A_c \cdot V_v \left[\frac{P^v_{PIN}}{P_{diff}} \cdot \frac{f_{ac}}{1-f_{av}} + \frac{1-f_{ac}}{1-f_{av}}\right]}, \qquad \text{(Eq.7')}$$

that shows that number of auxin molecules loaded inside the vesicle is proportional to P^v_{PIN}**.**

We can also rewrite this equation in the form:

$$N^{max}_v = A_c \cdot V_v \cdot R, \qquad \text{(Eq.7'')}$$

where

$$R = \frac{A^{max}_v}{A_c} = \frac{P^v_{PIN}}{P_{diff}} \cdot \frac{f_{ac}}{1 - f_{av}} + \frac{1 - f_{ac}}{1 - f_{av}} \qquad \text{(Eq.8)}$$

is the *accumulation ratio* – the ratio of intravesicular IAA concentration to that in the cytoplasm surrounding the vesicle. Expressions for accumulation ratio and maximum loading of vesicles for different pH_v are presented in Table 2.

Preprints (www.preprints.org) | NOT PEER-REVIEWED | Posted: 18 September 2018 doi:10.20944/preprints201809.0341.v1

Peer-reviewed version available at Int. J. Mol. Sci. 2018, 19, 3566; doi:10.3390/ijms19113566

1.4. Lower bound for accumulation ratio R necessary to produce the PAT.

In this section we estimated the auxin accumulation ratio R in vesicles, which is necessary to produce v_{PAT} if auxin in transported via vesicles *only*. Auxin flux density that corresponds to v_{PAT} velocity is given by

$$\Phi_{cell\to apoplast} = v_{PAT} \cdot A_c \ [\frac{mol}{\mu m^2 \cdot s}]. \quad \text{(Eq.9)}$$

Maximum flux of auxin, that vesicles can carry through the PM is

$$\Phi_v = N_v^{max} \cdot F_{max}^{+} \ [\frac{mol}{\mu m^2 \cdot s}], \quad \text{(Eq.10)}$$

where F_{max}^{+} is maximum exocytosis frequency (vesicles per second fusing with the unit area of cell face). This flux should be not lower than the yielded flux:

$$\Phi_v \geq \Phi_{cell\to apoplast}. \quad \text{(Eq.11)}$$

Thus,

$$N_v^{max} \cdot F_{max}^{+} \geq v_{PAT} \cdot A_c \quad \text{(Eq.12)}$$

which gives, using Eq. 7'':

$$R \cdot A_c \cdot V_v \cdot F_{max}^{+} \geq v_{PAT} \cdot A_c \quad \text{(Eq.12')}$$

Consequently,

$$R \geq \frac{v_{PAT}}{V_v \cdot F_{max}^{+}}. \quad \text{(Eq.13)}$$

Substituting F_{max}^{+} with its expression (see Eq.1.7 in Box 1) $F_{max}^{+} = \frac{ln2}{S_v \cdot \tau_{1/2}} \left(\frac{\rho_{PM}}{\rho_v}\right)_{max}$, we can find the lower bound of the accumulation ratio, that is required for v_{PAT}:

$$\boldsymbol{R \geq \frac{v_{PAT} \cdot S_v \cdot \tau_{1/2}}{V_v \cdot ln2} \left(\frac{\rho_v}{\rho_{PM}}\right)_{min}}. \quad \text{(Eq.14)}$$

Note, that intracellular auxin concentration A_c cancels (Eq.12'), that means that the equations are valid for any A_c. Nevertheless, we checked that vesicles will contain at least one molecule of auxin for the physiological value of A_c – a condition required for auxin transport to be theoretically possible (see Box 3). We also calculated minimum accumulation ratio required for $v_{PAT} = 1\ \mu m/s$ (Box 3).

Box.1. Expression for F^+, frequency of secretory vesicles fusing with PM, and estimation of its maximum value F_{max}^{+}.

In the following text we will consider only the polar domain of PM, which is the front membrane in the direction of PAT. It contains more PINs than the neighboring sides of the PM, and is visible by fluorescence microscopy [19]. The density of PINs depends on the rate of their delivery to PM by vesicles and on the rate of their removal. We assume that within the polar domain PINs are homogeneously distributed. Mass conservation for number of PINs on a polar domain of PM membrane of area S_{PM} then reads:

$$\frac{dn}{dt} = n_v F^+ S_{PM} - \beta \cdot n, \quad \text{(Eq.1.1)}$$

where n - number of PINs on PM, n_v - number of PINs in one vesicle, F^+ is frequency of exocytosis. PINs come to PM via $F^+ S_{PM}$ vesicles per second. Removal of PINs is proportional to n with the decay coefficient β, which describes any possible mechanism (through endocytosis, diffusion to other PM domains, degradation etc.).

If exocytosis is stopped, $F^+ = 0$, PINs are only removed:

Preprints (www.preprints.org) | NOT PEER-REVIEWED | Posted: 18 September 2018 doi:10.20944/preprints201809.0341.v1

Peer-reviewed version available at Int. J. Mol. Sci. 2018, 19, 3566; doi:10.3390/ijms19113566

$$\frac{dn}{dt} = -\beta \cdot n. \quad \text{(Eq.1.2)}$$

The solution of this equation reads:

$$n(t) = n(0)e^{-\beta \cdot t} \quad \text{(Eq.1.3)}$$

Introducing half-life $\tau_{1/2}$, time when 50% of PINs has been removed ($n(\tau_{1/2}) = n(0)/2$), gives β:

$$\beta = \frac{ln2}{\tau_{1/2}}. \quad \text{(Eq.1.4)}$$

At steady state, when removal and arrival of PINs are balanced, $\frac{dn}{dt} = 0$,

$$n_v F^+ S_{PM} = \beta \cdot n. \quad \text{(Eq.1.5)}$$

Eq.1.4 and Eq.1.5 give us expression for F^+, the frequency of vesicle fusion with the PM:

$$F^+ = \frac{ln2}{S_{PM} \cdot \tau_{1/2}} \frac{n}{n_v}, \quad \text{(Eq.1.6)}$$

We rewrite it using $\rho_{PM} = \frac{n}{S_{PM}}$, $\rho_v = \frac{n_v}{S_v}$ - densities of PINs on the PM and vesicle membrane respectively:

$$F^+ = \frac{ln2}{S_{PM} \cdot \tau_{1/2}} \frac{n}{n_v} = \frac{ln2}{S_{PM} \cdot \tau_{1/2}} \frac{\rho_{PM}}{\rho_v} \frac{S_{PM}}{S_v} = \frac{ln2}{S_v \cdot \tau_{1/2}} \frac{\rho_{PM}}{\rho_v} \quad \text{(Eq.1.7)}$$

$\tau_{1/2} = 1.3 \cdot 10^4 s$, which has been measured by Jásik et al. ([19]) for PIN2 in epidermal cells of Arabidopsis root. Finally, introducing values for S_v and $\tau_{1/2}$ gives:

$$F^+ = \frac{0.69}{1.1 \cdot 10^{-2}\ \mu m^2 \cdot 1.3 \cdot 10^4\ s} \frac{\rho_{PM}}{\rho_v} = \frac{\rho_{PM}}{\rho_v} \cdot 0.005 \frac{1}{\mu m^2\ s}, \quad \text{(Eq.1.8)}$$

Introducing estimation of minimum value for densities ratio $\left(\frac{\rho_v}{\rho_{PM}}\right)_{min} = 0.01$ (see Box.2) into Eq.1.8 gives upper bound for F^+:

$$F^+_{max} = 0.5 \frac{vesicles}{\mu m^2\ s}. \quad \text{(Eq.1.9)}$$

Experimentally measured endocytosis rate gives alternative estimate of exocytosis rate.

In accordance with the above result, the measured rate of endocytosis is $\sim 0.5 \frac{vesicles}{\mu m^2\ s}$ (Table 3). The total area of vesicles fusing with the PM in one cell has to be balanced by the area of endocytosed vesicles. Given that sizes of exocytotic and endocytotic vesicles are the same, maximal rate of endocytosis gives a rough estimate of maximal possible rate of exocytosis, which is in the same order of magnitude as our theoretical estimate.

It is worth to note that the half-life of PINs $\tau_{1/2}$ was measured for "old" PINs and doesn't account for possibility of "old" PINs being removed and brought back to the membrane via vesicles. This process would effectively reduce $\tau_{1/2}$ and allow for higher F^+_{max}. However, based on our comparison with experimental values of endocytosis, we argue that F^+_{max} can not be much higher than $0.5 \frac{vesicles}{\mu m^2\ s}$. This restriction comes from physiological *in vivo* rate of endocytic vesicle formation (taking ~18-22 seconds per vesicle, see Table 3 and [21]) and limited area of the cell membrane.

Box.2. Estimation of minimal PINs density ratio on vesicles and PM: $\left(\frac{\rho_v}{\rho_{PM}}\right)_{min}$.

The lowest possible density of PINs on the vesicular membrane is one PIN molecule per vesicle: $(\rho_v)_{min} = \frac{1}{S_v} = 50 \frac{1}{\mu m^2}$.

Preprints (www.preprints.org) | NOT PEER-REVIEWED | Posted: 18 September 2018 doi:10.20944/preprints201809.0341.v1

Peer-reviewed version available at *Int. J. Mol. Sci.* **2018**, *19*, 3566; doi:10.3390/ijms19113566

The maximum PIN density can be calculated as follows: diameter of the globular 60kDa protein is ~ 8nm. If PINs on the PM are densely packed, their density is at most $(\rho_{PM})_{max} \cong 2 \cdot 10^4 \frac{1}{\mu m^2}$, which is the maximum value of PIN density on PM.

Thus,

$$\left(\frac{\rho_v}{\rho_{PM}}\right)_{min} = \frac{(\rho_v)_{min}}{(\rho_{PM})_{max}} = 0.002. \quad \text{(Eq.2.1)}$$

However, PINs most probably cannot reach this maximum density in vivo, for the reason that numerous other proteins occupy space in the membrane. Also quantification of PIN2-GFP in epidermal cells of Arabidopsis root cells, observed using 3D structure illumination microscopy (SIM) with a resolution of 110 nm (Figure 3a), showed that separated source-spots of GFP signal are always resolved with maximum density of $5.6 \frac{spots}{\mu m^2}$ (Figure 3b). Each of the spot contains at least one PIN-GFP protein. However, most spots are large: mean area of the spots is $0.034 \pm 0.002\ \mu m^2$, max area $0.098\ \mu m^2$, min area $0.01\ \mu m^2$ (corresponds to resolution limit). Thus, most spots are likely to contain many PINs, which all together fill at most 1/5 part of the membrane area (as $5.6 \frac{1}{\mu m^2} \cdot 0.034\ \mu m^2 = 0.19$). This result argues that upper bound for the PIN density on PM is less than close-packing: $(\rho_{PM})_{max} \leq 4 \cdot 10^3 \frac{1}{\mu m^2}$. Correspondingly,

$$\left(\frac{\rho_v}{\rho_{PM}}\right)_{min} = \mathbf{0.01} \quad \text{(Eq.2.2)}$$

is a more realistic value of minimal PINs density ratio for epidermal root cells.

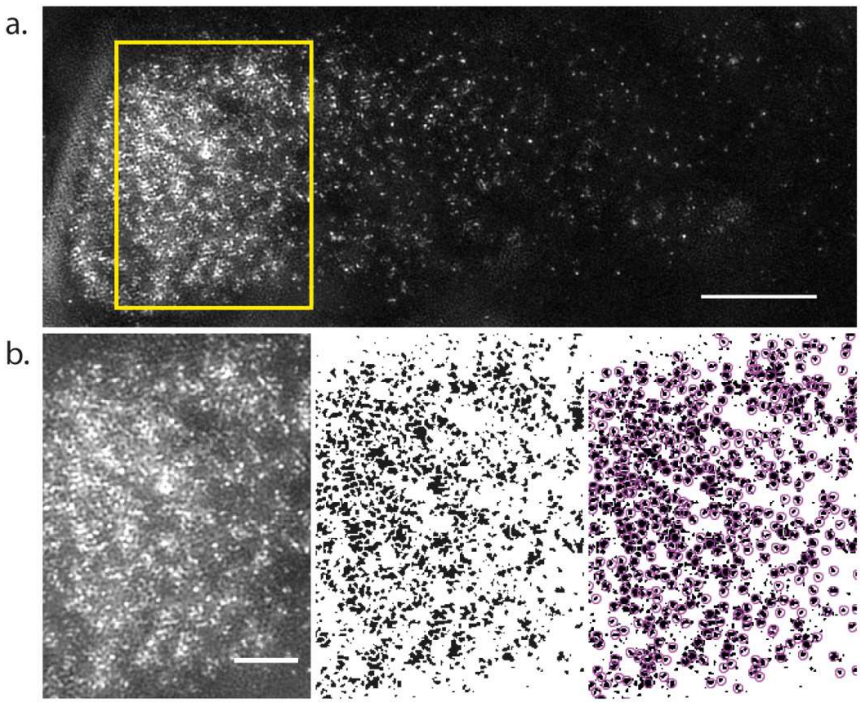

Figure 3. PIN2-GFP density measured by 3D SIM. **(a)** Example max projection of a 3D SIM image of the lateral membrane of root epidermal cells. **(b)** Left panel; magnified of the yellow rectangle in (a). Middle panel; the image is made binary and subjected to watershed segmentation. Right panel; pink circles denote detected PIN2-GFP spots. Scale bars; a, 5 μm, b, 2 μm..

Preprints (www.preprints.org) | NOT PEER-REVIEWED | Posted: 18 September 2018 doi:10.20944/preprints201809.0341.v1

Peer-reviewed version available at Int. J. Mol. Sci. 2018, 19, 3566; doi:10.3390/ijms19113566

Table 3. Calculation of rate of endocytosis (based on values from [22,23])

Endocytic marker	**DRP1C-GFP**	**CLC-GFP**
foci per μm²	3.54	3.48
SD	0.62	0.55
average lifetime (s)	17.7	19.7
SD	8.8	6.8
foci per model cell (15x15 micron)	796.5	783
SD	139.5	123.75
Endocytosis events per cell per second	**DRP1C-GFP**	**CLC-GFP**
Average	45.0	39.7
max	105.2	70.3
min	24.8	24.9
Maximum rate of endocytosis per second per μm²	**0.467**	**0.312**

Box 3. How many IAA molecules should be inside of one vesicle?

To find the accumulation ratio R, which is necessary for minimal PAT: $v_{PAT} = 1\frac{\mu m}{s}$. Rewriting Eq.14 as inequality gives:

$$\boldsymbol{R \geq \frac{v_{min}\, S_v \cdot \tau_{\frac{1}{2}}}{V_v \cdot ln2}\left(\frac{\rho_v}{\rho_{PM}}\right)_{min}} = \frac{1\frac{\mu m}{s}\, 2{\cdot}10^{-2}\mu m^2\, 1.3{\cdot}10^4\, s}{2.7{\cdot}10^{-4}\mu m^3 \cdot 0.69} 0.002 > \mathbf{2800} \qquad \text{(Eq.3.1)}$$

This minimal required accumulation ratio is valid for any A_c. Nevertheless, we have to check, that vesicles will contain at least one molecule. In the volume of a vesicle (maximum 2.7 x10⁵ nm³) there will be initially $N_v^{t=0} = A_c \cdot V_v = 0.005$ molecules if cytoplasmic auxin concentration $A_c = 30nM$, which is a plausible estimate for the root epidermis [24]. For the lowest possible accumulation ratio $R = 2800$ number of molecules in one vesicle will be $N_v = A_c \cdot V_v \cdot R \approx 14$, which is a minimal requirement for vesicular transport.

2. Minimal permeability of PINs in vesicles necessary for vesicular auxin transport.

By combining Eq.8 and Eq. 14, we can find the relation between vesicular PINs permeability P_{PIN}^{v-only} and the transport velocity v_{PAT} in the case that PINs are only active in vesicles and thus all PAT is produced by vesicles:

$$\frac{P_{PIN}^{v-onl}}{P_{diff}} \cdot \frac{f_{ac}}{1-f_{av}} + \frac{1-f_{ac}}{1-f_{av}} \geq \frac{v_{PAT}\, S_v \cdot \tau_{1/2}}{V_v \cdot ln2}\left(\frac{\rho_v}{\rho_{PM}}\right)_{min}$$

Consequently,

$$P_{PIN}^{v-onl} \geq P_{diff}\left(\frac{v_{PAT} \cdot S_v \cdot \tau_{1/2}}{V_v \cdot ln2}\left(\frac{\rho_v}{\rho_{PM}}\right)_{min} - \frac{1-f_{ac}}{1-f_{av}}\right) / \left(\frac{f_{ac}}{1-f_{av}}\right)$$

Preprints (www.preprints.org) | NOT PEER-REVIEWED | Posted: 18 September 2018 doi:10.20944/preprints201809.0341.v1

Peer-reviewed version available at Int. J. Mol. Sci. 2018, 19, 3566; doi:10.3390/ijms19113566

Thus, because $\frac{1-f_{ac}}{1-f_{av}}$ can be neglected being much smaller than the first term,

$$P_{PIN}^{v-only} \geq P_{diff} \cdot \frac{\mathrm{v}_{PAT} \cdot S_v \cdot \tau_{1/2}}{V_v \cdot ln2} \frac{(1-f_{av})}{f_{ac}} \left(\frac{\rho_v}{\rho_{PM}}\right)_{min} \quad \text{(Eq.15)}$$

From the Table 2 we find $min\left(\frac{1-f_{av}}{f_{ac}}\right) = 0.006$ for $pH_v = 7.0$, and using $\frac{\rho_v}{\rho_{PM}} = 0.01$ from Box.2, and parameter values from Table 1 we reduce inequality to

$$P_{PIN}^{v-only} \geq 80 \frac{s}{\mu m} \cdot \mathrm{v}_{PAT} \cdot P_{diff} \quad \text{(Eq.16)}$$

Diffusional permeability has been measured: $P_{diff} = 0.5$ μm/s. This gives an estimate of the lower bound of PIN permeability in vesicles:

$$\boldsymbol{P_{PIN}^{v-only} \geq 40 \cdot \mathrm{v}_{PAT}} \quad \text{(Eq.17)}$$

For $pH_v < 7.0$ bounds for $\frac{P_{PIN}^{v-onl}}{P_{diff}}$ are provided in Table 2. For pH value that we consider realistic, $pH_v = 6.2$ permeability has to be higher: $P_{PIN}^{v-onl} \geq 260 \cdot \mathrm{v}_{PAT}$.

3. Membrane permeability due to PINs has to be much greater on the vesicles than on PM to produce the same auxin transport velocity.

It would be informative to compare our estimate of the permeability value (Eq.17) $\boldsymbol{P_{PIN}^{v-only} \geq 40 \cdot \mathrm{v}_{PAT}}$ with experimental measurements. Unfortunately, the permeability of PINs has never been measured directly in the intact tissues. Also measurements of the influx carrier permeability are not possible in explants like protoplasts, as PINs do not stay on the PM, but are instead internalized [25], resulting in no contribution to the efflux of auxin as in vivo systems.

Fortunately, analogous estimates for PIN permeability have been done for the case when PINs are active only on PM (see Box.4, [17]), which have been shown that:

$$\boldsymbol{P_{PIN}^{PM-only} \simeq \mathrm{v}_{PAT}} \quad \text{(Eq.18)}$$

This relation was proved in theoretical studies using simple mathematical models and confirmed by computational models of multicellular tissues (see Box.4). It is determined under the assumption that PINs are active only on the PMs and facilitate auxin transport without any action from vesicles. Consequently, in epidermal cells of Arabidopsis root $P_{PIN2}^{PM} \simeq 1$ μm/s.

We conclude from Eq.18 and Eq.19 that if all other parameters are held in physiological range, to yield the same PAT velocity as PM PINs, vesicular PINs permeability has to be much higher: $\frac{P_{PIN}^{v-only}}{P_{PIN}^{PM-only}} \geq 40$. However, P_{PIN}^{v-onl} and P_{PIN}^{PM-on} also depend on density of PINs on the membranes. To clarify this issue, in the next section we calculated the ratio of PINs activity, which is characteristic of individual transporters and which does not depend on the densities of PINs.

Box.4. The permeability of PINs on the plasma membrane $\boldsymbol{P_{PIN}^{PM}}$ equals the directional auxin transport velocity $\boldsymbol{\mathrm{v}_{PAT}}$.

P_{PIN}^{PM} can be derived from the following considerations, analogous to Eq.9-11. Auxin flux density through plasma membrane has the following expression because PINs are transporting anions IAA^- and depend only on its intracellular concentration $f_{ac} \cdot A_C$ (=Eq.21):

$$\Phi_{PM} = P_{PIN}^{PM} \cdot f_{ac} \cdot A_C \quad \text{(Eq.4.1)}$$

It should be equal to PAT flux (Eq.9): $\Phi_{PM} = \Phi_{cell \to apoplast}$. Thus,

Preprints (www.preprints.org) | NOT PEER-REVIEWED | Posted: 18 September 2018 doi:10.20944/preprints201809.0341.v1

Peer-reviewed version available at Int. J. Mol. Sci. 2018, 19, 3566; doi:10.3390/ijms19113566

$$P_{PIN}^{PM} \cdot f_{ac} \cdot A_C = \mathrm{v}_{PAT} \cdot A_c \quad \text{(Eq.4.2)}$$

Consequently,

$$\boldsymbol{P_{PIN}^{PM} \cong \mathrm{v}_{PAT}} \quad \text{(Eq.4.3)}$$

Thus, for $\mathrm{v}_{PAT} = 1$ μm/s, $P_{PIN}^{PM} = 1$ μm/s.

In fact, [16] and [26] have shown that for a file of cells transport speed is comparable to the efflux permeability, and this conclusion was confirmed by computer simulations of multilayered tissues [16],[17],[26]. In these classical works, it has been proven that "advection" of auxin can be just a result of combined polar membrane transport and cytoplasmic diffusion. Thus, macroscopic advection velocity is limited either by polar membrane transport or by the rate of auxin's transfer along the cell length; whichever value is lower. One can calculate that diffusion along the longest cell length (~ 100 μm) is faster than the measured velocity, proving that cytoplasmic transport does not limit the "macroscopic advection velocity v_{PAT}" [13]. In this case, polar membrane transport governs macroscopic velocity [16][26]. To show this we provide derivation done by Mitchison [16].

Derivation of P_{PIN}^{PM} that would yield $\mathrm{v}_{PAT} = 1$ μm/s from theory developed by Mitchison[16]**.**

Equation (2) from reads [16]:

$$\frac{1}{\mathrm{v}_{PAT}} = \frac{1}{p} + \left(1 + \frac{2q}{p}\right)\frac{L}{2D},$$

where v_{PAT} – macroscopic auxin velocity, p – polar efflux permeability, q – nonpolar permeability (by diffusion), L- cell length, D- diffusion coefficient of auxin inside the cell. Because $\frac{L}{2D} \leq \frac{1 \cdot 10^{-4} m}{2 \cdot 6.7 \cdot \frac{10^{-1}\ m^2}{s}} = 7.46 \cdot 10^{-4} s/m$, $\mathrm{v}_{PAT} = 1 \cdot 10^{-6} m/\mathrm{s}$ and $q \geq 0$,

$$\Rightarrow \boldsymbol{p = \frac{1 + 2q\frac{L}{2D}}{\frac{1}{\mathrm{v}_{PAT}} - \frac{L}{2D}} \geq 1.1 \cdot 10^{-6} m/s}\,.$$

This equation also shows that the lower bound of efflux permeability $p \cong \mathrm{v}_{PAT}$, because $\frac{L}{2D} \ll 1$. Note, that condition $\frac{1}{\mathrm{v}_{PAT}} - \frac{L}{2D} \geq 0$ must hold, so that value of permeability is positive, which is true for $\mathrm{v}_{PAT} \leq \frac{2D}{L} = 13.4 \cdot 10^{-6} m$. Estimates of permeability values provided by [16] are in the same order of magnitude.

In principle, auxin-containing vesicles can also contribute to directional transport within the cell. However, as noted above, diffusion is already sufficient to transport auxin inside the cell, so such additional "acceleration" is not relevant for the macroscopic transport rate.

4. Individual activity of PINs has to be much higher on the vesicles than on the PM to produce the same auxin transport velocity.

To compare the efficiency of transport it is necessary to normalize permeabilities P_{PIN}^{v-only} and $P_{PIN}^{PM-only}$ to the corresponding density of PINs. The ratio of normalized permeabilities equals the ratio of individual activity of PIN transporters situated in vesicles ($\boldsymbol{p_{v-only}}$) and on the PM ($\boldsymbol{p_{PM-only}}$) (see Box.5 for explanation): $\frac{p_{v-on}}{p_{PM-only}} = \frac{P_{PIN}^{v-only}}{\rho_v} \frac{\rho_{PM}}{P_{PIN}^{PM-only}}$.

Combining this equation (=Eq. 5.1), and Eq. 15(equality form)

$$P_{PIN}^{v-only} = P_{diff} \cdot \frac{\mathrm{v}_{PAT} \cdot S_v \cdot \tau_{1/2}}{V_v \cdot ln2} \frac{(1 - f_{av})}{f_{ac}} \frac{\rho_v}{\rho_{PM}}$$

Preprints (www.preprints.org) | NOT PEER-REVIEWED | Posted: 18 September 2018 doi:10.20944/preprints201809.0341.v1

Peer-reviewed version available at Int. J. Mol. Sci. 2018, 19, 3566; doi:10.3390/ijms19113566

gives:

$$\frac{p_{v-only}}{p_{PM-only}} = \frac{v_{PAT} \cdot S_v \cdot \tau_{1/2}}{V_v \cdot ln2} \frac{\rho_v}{\rho_{PM}} \cdot \frac{P_{diff}}{P_{PIN}^{PM-on}} \cdot \frac{\rho_{PM}}{\rho_v} \frac{1-f_{av}}{f_{ac}}.$$

Note, that density ratio $\frac{\rho_v}{\rho_{PM}}$ cancels in this equation:

$$\frac{p_{v-onl}}{p_{PM-on}} = \frac{v_{PAT} \cdot S_v \cdot \tau_{1/2}}{V_v \cdot ln2} \cdot \frac{P_{diff}}{P_{PIN}^{PM-only}} \cdot \frac{1-f_{av}}{f_{ac}}$$

By calculating the minimum of the right-hand side we can find the lower bound for PINs activity ratio.

$$\frac{p_{v-only}}{p_{PM-only}} \geq \left(\frac{v_{PAT} S_v \cdot \tau_{\frac{1}{2}}}{V_v \cdot ln2} \cdot \frac{P_{diff}}{P_{PIN}^{PM-only}} \cdot \frac{1-f_{av}}{f_{ac}} \right)_{min} \quad \text{(Eq.19)}$$

Using the fact that $v_{PAT} \cong P_{PIN}^{PM-only}$ (see Box.4) we find[1]:

$$\frac{p_{v-only}}{p_{PM-only}} > \mathbf{4200}. \quad \text{(Eq.20)}$$

For $pH_v = 6.2$, (see Table 2), the ratio is even higher: $\frac{p_{v-only}}{p_{PM-only}} > 26600$.

Conclusion I: For vesicle transport to be able to produce all of the observed IAA flux, the activity of PINs on the vesicle membrane has to be at least three orders of magnitude greater than that estimated for the case when PINs are only active on the PM. Our calculations show that transporting auxin directly through the PM is 1000 times more effective than by means of SVs. This, in our opinion, is an argument against SVs-mediated transport of auxin as a major mechanism of directional auxin transport.

Box. 5. Individual activity (specific permeability) of PIN transporters.

Membrane permeability due to PINs is proportional to PINs density and can be expressed as a product of 1) density of transporters on the membrane ρ_{PIN} $[\frac{\text{mol}}{\mu\text{m}^2}]$ and 2) individual activity of one transporter protein $p_{PIN}[\frac{\mu\text{m/s}}{\text{mol}/\mu\text{m}^2}]$, which depends on affinity to auxin, electrical potential across the membrane*, phosphorylation status and any other parameters.

$$P_{PIN} = \rho_{PIN} \cdot p_{PIN} \quad \text{(Eq.5.1)}$$

* Dependence on membrane potential has been derived in [26]): $p_{PIN}(\Delta V) \sim \frac{\Delta V \cdot F/\mathcal{R}T}{\exp\left(\frac{F \cdot \Delta V}{\mathcal{R}T}\right)-1}$, where F is the Faraday constant, $\mathcal{R}$ is the gas constant, T is the temperature. For the plasma membrane $\Delta V \sim -160 \div -100$mV. For exocytotic vesicles it is unknown.

2.3.2. PINs active both in vesicles and on PM

Next, we find the ratio of auxin fluxes through both mechanisms in the case that PINs are active on vesicles and the PM. Auxin efflux caused by (active) PINs on the PM:

$$\Phi_{PM} = P_{PIN}^{PM} \cdot f_{ac} \cdot A_C. \quad \text{(Eq.21)}$$

Auxin efflux caused by arriving PIN delivery vesicles (using Eq.7′):

[1] $\left(\frac{\cancel{v_{PAT}} S_v \cdot \tau_{\frac{1}{2}}}{V_v \cdot ln2} \cdot \frac{P_{diff}}{\cancel{P_{PIN}^{PM}}} \cdot \frac{1-f_{av}}{f_{ac}} \right)_{min} = \frac{10^2 \cdot 6 \cdot 1.3 \cdot 10^4}{8 \cdot 0.69} \cdot \frac{6 \cdot 10^{-3}}{2} \cong 4200$.

Preprints (www.preprints.org) | NOT PEER-REVIEWED | Posted: 18 September 2018 doi:10.20944/preprints201809.0341.v1

Peer-reviewed version available at Int. J. Mol. Sci. 2018, 19, 3566; doi:10.3390/ijms19113566

$$\Phi_v = N_v \cdot F^+ \cong \frac{P_{PIN}^v}{P_{diff}} \cdot \frac{f_{ac}}{1-f_{av}} \cdot V_v \cdot F^+ \cdot A_c. \quad \text{(Eq.22)}$$

Dividing Eq.21 by Eq. 22 gives flux ratio:

$$\frac{\Phi_{PM}}{\Phi_v} = \frac{P_{PIN}^{PM} \cdot f_{ac} A_c}{\frac{P_{PIN}^v}{P_{diff}} \frac{f_{ac}}{1-f_{av}} V_v \cdot F^+ \cdot A_c} = \frac{P_{PIN}^{PM}}{P_{PIN}^v} \cdot \frac{P_{diff}(1-f_{av})}{V_v} \cdot \frac{1}{F^+}. \quad \text{(Eq.23)}$$

Substituting F^+ by its expression from Eq.1.7 gives:

$$\frac{\Phi_{PM}}{\Phi_v} = \frac{P_{PIN}^{PM}}{P_{PIN}^v} \cdot \frac{P_{diff} \cdot (1-f_{av})}{V_v} \frac{\rho_v}{\rho_{PM}} \frac{S_v \cdot \tau_{1/2}}{ln2}. \quad \text{(Eq.23')}$$

Using Eq.5.1 we reduce it further:

$$\frac{\Phi_{PM}}{\Phi_v} = \frac{P_{diff} \cdot (1-f_{av})}{V_v} \frac{S_v \cdot \tau_{1/2}}{ln2} \cdot \frac{\boldsymbol{p_{PM}}}{\boldsymbol{p_v}}. \quad \text{(Eq.24)}$$

Introducing parameter values for pH=7 and d=0.08 μm gives a lower bound on the ratio:

$$\frac{\boldsymbol{\Phi_{PM}}}{\boldsymbol{\Phi_v}} \geq \mathbf{4200} \cdot \frac{\boldsymbol{p_{PM}}}{\boldsymbol{p_v}}. \quad \text{(Eq.25)}$$

where $\frac{\boldsymbol{p_{PM}}}{\boldsymbol{p_v}}$ is the ratio of individual PINs activity (see Box.5) on the PM and vesicles if PINs are active on both membranes. Note, that the densities of PINs cancel, and flux distributions between the two mechanisms depends only on the activity of PINs.

If the individual activity of PINs on the vesicle and on membrane are equal ($\mathbf{p_v} = \mathbf{p_{PM}}$), then

$$\frac{\boldsymbol{\Phi_{PM}}}{\boldsymbol{\Phi_v}} \geq \mathbf{4200}, \quad \text{(Eq.26)}$$

which means that the flux through the vesicle mechanism does not contribute more than 0.02% to the total flux.

For $pH_v = 6.2$ the lower bound of the ratio is higher: $\frac{\Phi_{PM}}{\Phi_v} \geq 26600$, which implies that the contribution of the vesicular mechanism is less than 0.004%, which is negligibly small compared to PM flux.

The flux ratio $\frac{\Phi_{PM}}{\Phi_v}$ would be higher (favoring PM flux over SV-mediated flux) if:

- PINs half-life on PM is higher
- pH in vesicle is lower
- vesicles do not stay in the cytoplasm for enough time before fusing with the PM to be fully filled with IAA
- size of vesicles is smaller

The opposite changes of parameter values would increase SV-mediated contribution to the auxin flux (see Eq.24).

Conclusion II: The activity of PIN transporters in the vesicle has to be at least 1000 times greater than on the PM to make a substantial contribution to the total directional auxin transport. When realistic physiological parameter values were used in the model, a factor greater than 10^4 was determined.

3. Discussion

The hypothesis of vesicular secretion of auxin was postulated more than 15 years ago [6,7]. While several studies have claimed to provide experimental evidence to support this concept since [8–10], their conclusions are currently greatly debated in the field [11,12]. Hence the question whether vesicular secretion significantly contributes to intercellular auxin transport remains unresolved. Here, we took a modeling approach to estimate whether such a mode of auxin transport is even theoretically possible.

First, we compared individual activities of PINs active exclusively on vesicles or on the PM, that are necessary to yield the same PAT velocity (Eq.20):

Preprints (www.preprints.org) | NOT PEER-REVIEWED | Posted: 18 September 2018 doi:10.20944/preprints201809.0341.v1

Peer-reviewed version available at Int. J. Mol. Sci. 2018, 19, 3566; doi:10.3390/ijms19113566

$$\frac{p_{v-only}}{p_{PM-only}} \geq P_{diff}\left(\frac{6\cdot\tau_{1/2}}{d\cdot ln2}\cdot\frac{1-f_{av}}{f_{ac}}\right)_{min}. \quad \text{(Eq.27)}$$

This ratio is valid for any PAT velocity and depends on the following measurable parameters: diameter of vesicles d, half-life time of PINs on the PM $\tau_{1/2}$, pH-dependent fraction of IAAH in a vesicle $(1-f_{av})$, fraction of IAA^- in cytoplasm. Experimental parameter values (Table 1) gave us $\frac{p_{v-onl}}{p_{PM-only}} > 4200$, meaning that individual activity of PINs on SVs (p_v) needs to be at least three orders of magnitude greater than the activity of PINs on the PM (p_{PM}) in order to produce the same auxin transport.

We also provide an estimate for the permeability of PINs in the vesicles required to yield $v_{PAT} = 1\frac{\mu m}{s}$ in epidermal root cells: $P^v_{PIN} \geq 40\frac{\mu m}{s}$, which is not the measure of individual transporters, but characteristic of the unit area of membrane (explained in Box.5). This value is much higher than any measured permeabilities to date [17,20]. The measurements of permeability due to PINs either on the PM, in vesicles or in both domains will allow one to draw precise conclusions from our model.

To extend these findings further to a more general case, we derived an expression that relates auxin flux driven by PINs on the polar domain of PM and auxin flux driven by PINs at the vesicles, if they are both active (Eq.24):

$$\frac{\Phi_{PM}}{\Phi_v} = \frac{P_{diff}\cdot(1-f_{av})}{d}\cdot\frac{6\cdot\tau_{1/2}}{ln2}\cdot\frac{\boldsymbol{p_{PM}}}{\boldsymbol{p_v}}. \quad \text{(Eq.28)}$$

It shows that relative auxin fluxes through both mechanisms depend on: diameter of vesicles d, half-life time of PINs on the PM $\tau_{1/2}$, pH-dependent fraction of IAAH in a vesicle $(1-f_{av})$ and individual activities of PIN proteins p_{PM} and p_v.

The main parameter, namely PIN activity, has not been experimentally determined on the PM or in vesicles, which makes it impossible to find actual ratio of fluxes *in vivo*. Nevertheless, by estimating the extreme values of the rest of parameters from available experimental data (Table 1), we were able to show that $\frac{\Phi_{PM}}{\Phi_v} > 4200\cdot\frac{p_{PM}}{p_v}$. This expression suggests that if PINs were equally active both at the PM and on the SVs, the contribution of secreted IAA to the overall net IAA flux would be less than 0.02% at pH=7 inside vesicles of maximal size, which is the maximal possible contribution in that case.

Moreover, instead of the half-life time of PINs on the PM $\tau_{1/2}$ and vesicle diameter, other measurable parameters can be put in this equation (using Eq.1.7): exocytosis frequency F^+, densities of PINs $\rho_{v,PM}$ and vesicular volume V_v. Then Eq. 28 takes the following form:

$$\frac{\Phi_{PM}}{\Phi_v} = \frac{P_{diff}\,(1-f_{av})}{V_v}\cdot\frac{1}{F^+}\frac{\rho_v}{\rho_{PM}}\frac{\boldsymbol{p_{PM}}}{\boldsymbol{p_v}}, \quad \text{(Eq.29)}$$

We provide measurement of density of PINs $\rho_{PM} \leq 4\cdot 10^3\frac{1}{\mu m^2}$, which gives a plausible estimate of $\left(\frac{\rho_v}{\rho_{PM}}\right)_{min} = 0.01$ (Box 2). We also used published experimental data to estimate $F^+_{max} = 0.5\frac{vesicles}{\mu m^2\, s}$ (end of Box.1). These parameter values give the lower bound for flux ratios: $\frac{\Phi_{PM}}{\Phi_v} > 4200\cdot\frac{p_{PM}}{p_v}$, which coincide with the result in the previous paragraph. Thus, by acquiring the same minimal flux ratio using two different sets of parameters we confirm that our conclusions are plausible.

The fact that the parameter values can depend on cell type, PIN type or biochemical status of the cell, it is important to consider if in different tissue types vesicular transport can become dominant. Our equations can be used to resolve this question by calculating the auxin flux ratio for any other tissue type once experimental values are available; especially if the activity of individual PINs on the PM and on vesicles can be measured in the future. If it is found that PINs transporters are active exclusively in vesicles and are inactive on the PM ($p_{PM} = 0$) Eq.28&29 would become meaningless. This however remains a technically demanding value to determine experimentally. If it was found that PINs are active only on the vesicles, the testable relation between the individual activity of PINs and the measurable parameters is (from Eq.15):

$$p_{v-only} = \frac{P^{v-only}_{PIN}}{\rho_v} = \frac{P_{diff}}{\rho_{PM}}\cdot\frac{v_{PAT}\cdot 6\cdot\tau_{1/2}}{d\cdot ln2}\frac{(1-f_{av})}{f_{ac}}, \quad \text{(Eq.30)}$$

Preprints (www.preprints.org) | NOT PEER-REVIEWED | Posted: 18 September 2018 doi:10.20944/preprints201809.0341.v1

Peer-reviewed version available at Int. J. Mol. Sci. 2018, 19, 3566; doi:10.3390/ijms19113566

Notably, other parameters in Eq.28&29 cannot have zero values, thus, their change by orders of magnitude is needed to make vesicular auxin transport a dominant mechanism. Methods for separate perturbation of those parameters are needed to distinguish between vesicular-mediated and PM-mediated auxin fluxes.

In conclusion, we have created a simple mathematical model to calculate the efficiency of PIN-mediated vesicular secretion of auxin compared to transport across the PM. Even under the most "vesicular transport-favoring" values of the parameters the vesicular transport of auxin were still determined to be several orders of magnitude less efficient compared to the membrane transport. Our calculations showed that PINs on the PM can produce auxin transport having much less individual activity than required for PINs in the secretory vesicles (SVs). Therefore, we consider it unlikely that PINs are active only in the secretory vesicles; and in case they are active on both PM and SVs, vesicular transport would play a negligible role in PAT.

4. Materials and Methods

4.1.Measurement of PIN density using SIM

Samples were prepared as previously described by Johnson & Vert [21], where the imaging media was supplemented with 30% opti-prep and the coverslips were fixed on to the microscope slide. Cells in the elongation zone were imaged using an OMX v4 3D SIM. A z-stack was created to image the lateral membrane of the PIN2 polar domain and a maximum projection of this was used for analysis. Images were made binary and subjected to watershed segmentation using Fiji [27]. PIN2 spots were then detected using TrackMate [28]. Density of PIN2, mean, maximum and minimum area of the PIN2 spots was calculated from on 12343 spots in 9 different cells from 3 independent roots.

Acknowledgements: We cordially thank František Baluška, Kees Boot, Bert van Duijn, Geneviève Hines, Kees Libbenga and Eric Kramer for their valuable input to the initial discussions that led to this work. These took place at the "Quantitative Biology of Auxin Transport" workshop at the Lorentz Center, Leiden, Netherlands, 12-16 January 2015, we would therefore also like to acknowledge the organizers of this workshop.

We acknowledge the Advanced Microscopy Facility (advMICRO) of the Vienna Biocenter Core Facilities (VBCF), member of the Vienna Biocenter (VBC) Austria, for use of the OMX v4 3D SIM microscope.

Funding: M.A. was supported by the Austrian Science Fund (FWF) (M2379-B28). AJ was supported by the Austria Science Fund (FWF): I03630 to Jiri Friml.

Author contribution: Conceptualization, S.H., M.G and J.F.; Methodology, S.H., M.A., A.J.; Formal Analysis, S.H., M.A.; Investigation, S.H., M.A., M.G., A.J.; Visualization, S.H., A.J.; Funding Acquisition, S.H., J.F.; Writing – Original Draft Preparation, M.A., M.G.; Writing – Review & Editing, S.H., M.A., M.G., A.J., J.F.

Conflicts of Interest: The authors declare no conflict of interest.

Abbreviations

PM	plasma membrane
SV	secretory vesicle
IAA	3-indole acetic acid = auxin
PINs	PIN-formed transporters

References

1. Adamowski, M.; Friml, J. PIN-Dependent Auxin Transport: Action, Regulation, and Evolution. *Plant Cell Online* **2015**, *27* (1), 20–32, DOI.10.1105/tpc.114.134874.
2. Kleine-Vehn, J.; Langowski, L.; Wisniewska, J.; Dhonukshe, P.; Brewer, P. B.; Friml, J. Cellular and Molecular Requirements for Polar PIN Targeting and Transcytosis in Plants. *Mol. Plant* **2008**, *1* (6),

Preprints (www.preprints.org) | NOT PEER-REVIEWED | Posted: 18 September 2018 doi:10.20944/preprints201809.0341.v1

Peer-reviewed version available at Int. J. Mol. Sci. 2018, 19, 3566; doi:10.3390/ijms19113566

1056–1066, DOI.10.1093/mp/ssn062.

3. Geldner, N.; Friml, J.; Stierhof, Y.-D. D.; Jürgens, G.; Palme, K. Auxin Transport Inhibitors Block PIN1 Cycling and Vesicle Trafficking. *Nature* **2001**, *413* (6854), 425–428, DOI.10.1038/35096571.
4. Dhonukshe, P.; Aniento, F.; Hwang, I.; Robinson, D. G.; Mravec, J.; Stierhof, Y.-D. D.; Friml, J. J. Clathrin-Mediated Constitutive Endocytosis of PIN Auxin Efflux Carriers in Arabidopsis. *Curr. Biol.* **2007**, *17* (6), 520–527, DOI.10.1016/j.cub.2007.01.052.
5. Adamowski, M.; Narasimhan, M.; Kania, U.; Glanc, M.; De Jaeger, G.; Friml, J. A Functional Study of AUXILIN-LIKE1 and 2, Two Putative Clathrin Uncoating Factors in Arabidopsis. *Plant Cell* **2018**, tpc.00785.2017, DOI.10.1105/tpc.17.00785.
6. Friml, J.; Palme, K. Polar Auxin Transport – Old Questions and New Concepts ? *Plant Mol. Biol.* **2002**, *49*, 273–284.
7. Baluška, F.; Šamaj, J.; Menzel, D. Polar Transport of Auxin: Carrier-Mediated Flux across the Plasma Membrane or Neurotransmitter-like Secretion? *Trends Cell Biol.* **2003**, *13* (6), 282–285, DOI.10.1016/S0962-8924(03)00084-9.
8. Mancuso, S.; Marras, A. M.; Mugnai, S.; Schlicht, M.; Zársky, V.; Li, G.; Song, L.; Xue, H.-W.; Baluska, F. Phospholipase Dzeta2 Drives Vesicular Secretion of Auxin for Its Polar Cell-Cell Transport in the Transition Zone of the Root Apex. *Plant Signal. Behav.* **2007**, *2* (4), 240–244, DOI.10.4161/psb.2.4.4566.
9. Mettbach, U.; Strnad, M.; Mancuso, S.; Baluška, F. Immunogold-EM Analysis Reveal Brefeldin a-Sensitive Clusters of Auxin in Arabidopsis Root Apex Cells. *Commun. Integr. Biol.* **2017**, *10* (3), e1327105, DOI.10.1080/19420889.2017.1327105.
10. Schlicht, M.; Strnad, M.; Scanlon, M. J.; Mancuso, S.; Hochholdinger, F.; Palme, K.; Volkmann, D.; Menzel, D.; Baluska, F. Auxin Immunolocalization Implicates Vesicular Neurotransmitter-like Mode of Polar Auxin Transport in Root Apices. *Plant Signal. Behav.* **2006**, *1* (3), 122–133.
11. Alpi, A.; Amrhein, N.; Bertl, A.; Blatt, M. R.; Blumwald, E.; Cervone, F.; Dainty, J.; De Michelis, M. I.; Epstein, E.; Galston, A. W.; et al. Plant Neurobiology: No Brain, No Gain? *Trends Plant Sci.* **2007**, *12* (4), 135–136, DOI.10.1016/j.tplants.2007.03.002.
12. Robinson, D. G.; Hawes, C.; Hillmer, S.; Jürgens, G.; Schwechheimer, C.; Stierhof, Y.-D.; Viotti, C. Auxin and Vesicle Traffic. *Plant Physiol.* **2018**, *176* (3), 1884–1888, DOI.10.1104/PP.17.01510.
13. Kramer, E. M.; Rutschow, H. L.; Mabie, S. S. AuxV: A Database of Auxin Transport Velocities. *Trends in Plant Science*. Elsevier Current Trends September 2011, pp 461–463, DOI.10.1016/j.tplants.2011.05.003.
14. Petrášek, J.; Friml, J. Auxin Transport Routes in Plant Development. *Development* **2009**, *136* (16), 2675–2688, DOI.10.1242/dev.030353.
15. Rashotte, A. M.; Poupart, J.; Waddell, C. S.; Muday, G. K. Transport of the Two Natural Auxins, Indole-3-Butyric Acid and Indole-3-Acetic Acid, in Arabidopsis. *Plant Physiol.* **2003**, *133* (2), 761–772, DOI.10.1104/pp.103.022582.
16. Mitchison, G. J. The Dynamics of Auxin Transport. *Proc. R. Soc. B Biol. Sci.* **1980**, *209* (1177), 489–511, DOI.10.1098/rspb.1980.0109.
17. Rutschow, H. L.; Baskin, T. I.; Kramer, E. M. The Carrier AUXIN RESISTANT (AUX1) Dominates Auxin Flux into Arabidopsis Protoplasts. *New Phytol.* **2014**, *204* (3), 536–544, DOI.10.1111/nph.12933.
18. Pimpl, P.; Movafeghi, A.; Coughlan, S.; Denecke, J.; Hillmer, S.; Robinson, D. G. In Situ Localization and in Vitro Induction of Plant COPI-Coated Vesicles. *Plant Cell* **2000**, *12* (11), 2219–2236.

Preprints (www.preprints.org) | NOT PEER-REVIEWED | Posted: 18 September 2018 doi:10.20944/preprints201809.0341.v1

Peer-reviewed version available at Int. J. Mol. Sci. 2018, 19, 3566; doi:10.3390/ijms19113566

19. Jásik, J.; Boggetti, B.; Baluška, F.; Volkmann, D.; Gensch, T.; Rutten, T.; Altmann, T.; Schmelzer, E. PIN2 Turnover in Arabidopsis Root Epidermal Cells Explored by the Photoconvertible Protein Dendra2. *PLoS One* **2013**, *8* (4), e61403, DOI.10.1371/journal.pone.0061403.
20. Delbarre, A.; Muller, P.; Imhoff, V.; Guern, J. Comparison of Mechanisms Controlling Uptake and Accumulation of 2,4-Dichlorophenoxy Acetic Acid, Naphthalene-1-Acetic Acid, and Indole-3-Acetic Acid in Suspension-Cultured Tobacco Cells. *Planta* **1996**, *198* (4), 532–541, DOI.10.1007/BF00262639.
21. Johnson, A.; Vert, G. Single Event Resolution of Plant Plasma Membrane Protein Endocytosis by TIRF Microscopy. *Front. Plant Sci.* **2017**, *8*, 612, DOI.10.3389/fpls.2017.00612.
22. Konopka, C. a.; Bednarek, S. Y. Comparison of the Dynamics and Functional Redundancy of the Arabidopsis Dynamin-Related Isoforms DRP1A and DRP1C during Plant Development. *Plant Physiol.* **2008**, *147* (4), 1590–1602, DOI.10.1104/pp.108.116863.
23. Konopka, C. a.; Backues, S. K.; Bednarek, S. Y. Dynamics of Arabidopsis Dynamin-Related Protein 1C and a Clathrin Light Chain at the Plasma Membrane. *Plant Cell Online* **2008**, *20* (5), 1363–1380, DOI.10.1105/tpc.108.059428.
24. Fendrych, M.; Akhmanova, M.; Merrin, J.; Glanc, M.; Hagihara, S.; Takahashi, K.; Uchida, N.; Torii, K. U.; Friml, J. Rapid and Reversible Root Growth Inhibition by TIR1 Auxin Signalling. *Nat. Plants* **2018**, DOI.10.1038/s41477-018-0190-1.
25. Rutschow, H. L.; Baskin, T. I.; Kramer, E. M. The Carrier AUXIN RESISTANT (AUX1) Dominates Auxin Flux into Arabidopsis Protoplasts. **2014**.
26. Goldsmith, M. H.; Goldsmith, T. H.; Martin, M. H. Mathematical Analysis of the Chemosmotic Polar Diffusion of Auxin through Plant Tissues. *Proc. Natl. Acad. Sci. U. S. A.* **1981**, *78* (2), 976–980, DOI.10.1073/pnas.78.2.976.
27. Schindelin, J.; Arganda-Carreras, I.; Frise, E.; Kaynig, V.; Longair, M.; Pietzsch, T.; Preibisch, S.; Rueden, C.; Saalfeld, S.; Schmid, B.; et al. Fiji: An Open-Source Platform for Biological-Image Analysis. *Nat. Methods* **2012**, *9* (7), 676–682, DOI.10.1038/nmeth.2019.
28. Tinevez, J.-Y.; Perry, N.; Schindelin, J.; Hoopes, G. M.; Reynolds, G. D.; Laplantine, E.; Bednarek, S. Y.; Shorte, S. L.; Eliceiri, K. W. TrackMate: An Open and Extensible Platform for Single-Particle Tracking. *Methods* **2017**, *115*, 80–90, DOI.10.1016/j.ymeth.2016.09.016.